A TEM study of slip lines in power MOS devices

2000 J. Phys.: Condens. Matter 12 10279

(http://iopscience.iop.org/0953-8984/12/49/329)

J. Phys.: Condens. Matter **12** (2000) 10279–10286. Printed in the UK PII: S0953-8984(00)17580-0

A TEM study of slip lines in power MOS devices

A Rivière-Jérôme†, C Levade†, G Vanderschaeve†, I Percheron-Garçon‡ and B Forgerit‡

† CEMES–CNRS, 29 rue Jeanne Marvig, BP 4347, 31055 Toulouse Cedex, France
‡ Motorola, Le Mirail, BP 1029, 31023 Toulouse Cedex, France

Received 29 September 2000

Abstract. The defect structure of 'slip lines' in power MOS devices for automotive applications was investigated by means of selective chemical etching, atomic force microscopy (AFM) and transmission electron microscopy (TEM). Two different types of sample were investigated: (i) wafers taken after the epitaxy step and (ii) wafers that went through the whole process, thus containing operational devices. It is shown that a slip band contains an inhomogeneous density of dislocations, which probably interact with small defect clusters during their motion.

1. Introduction

The high temperature steps of silicon wafer processing often produce considerable mechanical and thermal stresses that induce dislocation formation [1]. Dislocations are known as being an important yield limiting factor in the production of integrated circuits. The aim of this study is to analyse those crystal defects that form slip bands in the silicon substrate and to establish a link with the electrical failure. Most of the previous observations were performed by means of x-ray topography [1] and combination of etching and copper decoration [2]. Stress tensor modelling was also used to determine the slip systems activated by the thermal stress in silicon crystals [3]. More recently, computer simulations were performed to estimate the slip band initiation location compared to x-ray topography [4]. We focus here on surface observations and on characterization of the dislocations using transmission electron microscopy.

The first part of this work is based on a comparison between a yield map and slip patterns. Figure 1(a) is a map of a silicon wafer obtained by electrically probing the dice. The bad dice (in black) present an electrical leakage between the drain and the source of the MOS transistor. The map shows that the bad dice are located in the corners, in the centre and near the flat part of the wafer (in the flat region, the border of the wafer indicates the [110] direction and laser marks are made to number the wafer). The observation of the surface by optical microscopy reveals the presence of so-called slip lines in ⟨110⟩ directions (figure 1(b)). A close correlation between slip line locations and the defective dice can be observed (figure 1(c)). These observations suggest that the generation of slip bands in the process is the probable cause of the device failure in agreement with similar statements reported in the literature [1].

The slip generation occurs during the first steps of integrated circuit manufacture (diffusion step and epitaxy step). In the course of the former step, the wafers are arranged in a furnace in such a way that they are subjected to a radial thermal gradient inducing a thermal stress [5]. In the epitaxy reactor, the wafers are laid on individual susceptors nearly vertically. In this case, the problem lies both in the temperature gradient of the susceptor that induce thermal stress

0953-8984/00/4910279+08$30.00

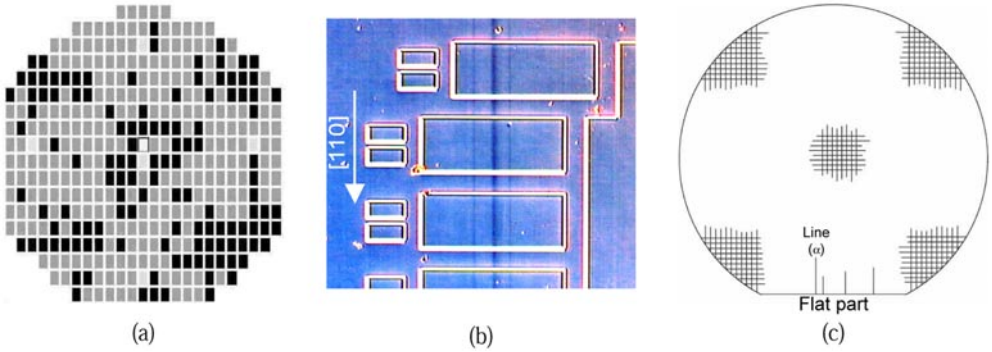

Figure 1. (a) Map obtained from electrical probing where the bad dice are in black, the good dice in grey and the test dice in white. (b) Optical microscopy observation of slip traces along [110]: the white contrast on the image comes from the buried layer pattern. (c) Location of the slip traces on a (001) wafer surface (schematics). Note the correlation between slip line location and the defective dice.

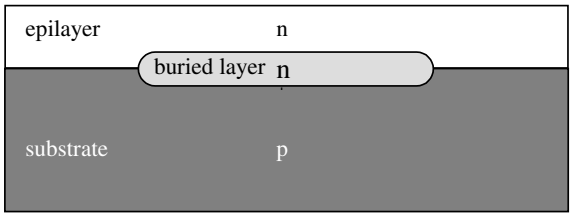

Figure 2. Schematic cross section of a wafer after the epitaxy step: p-type substrate, n^+-type buried layer, n-type epitaxy layer on top.

and in the gravitational stress of the wafer. When the stress exceeds the elastic limit of the silicon wafer, plastic deformation and stress relaxation occur via dislocation generation and glide, resulting in warpage of the wafer. Dislocation nucleation and propagation can also occur at microscratches [6], surface irregularities [1] and laser marks that act as stress concentrators.

2. Experimental method

2.1. Materials and process

The studied samples were ⟨001⟩ orientated silicon single crystals of 150 mm diameter grown by the Czochralski method and boron doped. Two types of sample were studied. (i) The first type were wafers taken directly from the production lines after the epitaxy step. They were p-type substrate, below an n^+-type buried layer with an n-type epitaxy layer on top. A schematic cross-section of a sample is given in figure 2. (ii) The second type of sample was wafers taken after the whole process and they contained many different layers (oxide, polysilicon, metal layers,. . .).

2.2. Surface analysis

Prior to TEM observations, surface characterizations were made on the wafers taken from the fabrication lines after the epitaxy step using both AFM and selective etching.

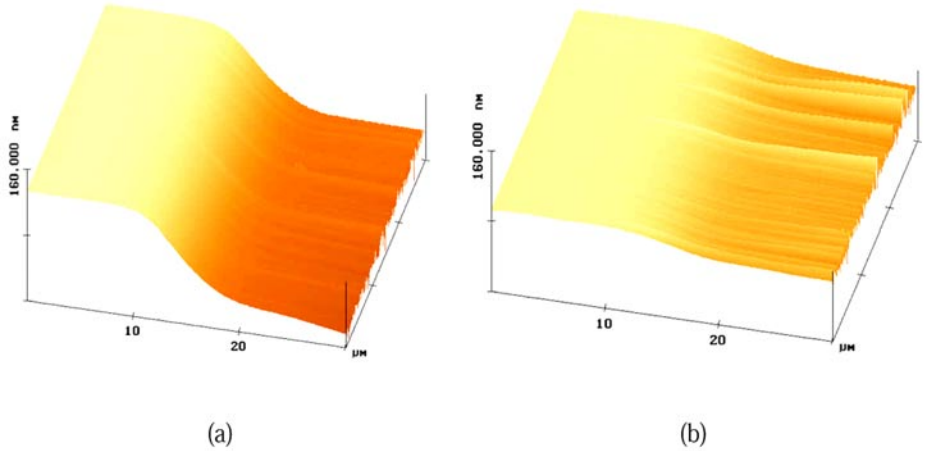

Figure 3. Surface topography by AFM in tapping mode perpendicularly to a visible slip line; (a) a region near the border of the wafer; (b) 1 cm away inside the wafer.

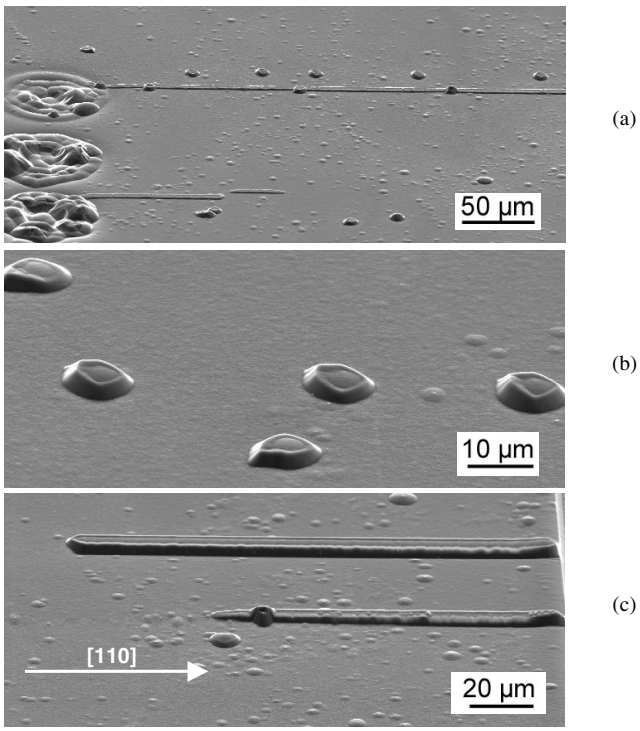

Figure 4. (a) Overview of etch mounds on a (001) silicon wafer aligned along the [110] direction; (b) individual mounds; (c) so many mounds that they cannot be distinguished.

2.2.1. Atomic force microscopy (AFM) observation. The wafer surface topography was studied by AFM (tapping mode). The surface was scanned by a probe perpendicularly to a visible slip trace in the region close to the flat part of a wafer like the slip line (α) in figure 1(c). The surface step due to the slip trace is higher near the border of the wafer (about 90 nm;

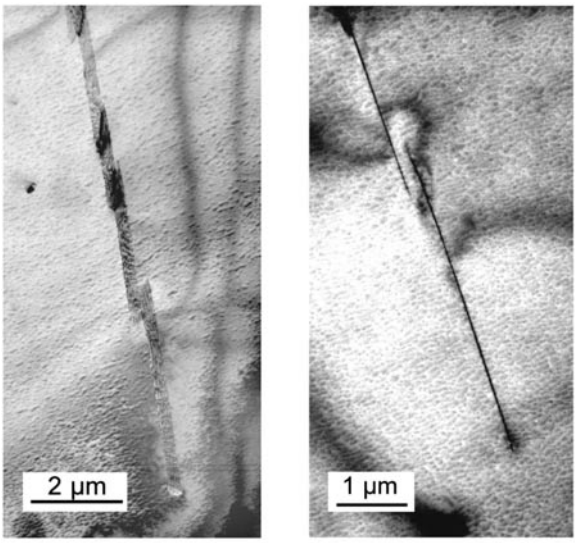

Figure 5. TEM bright field image of a slip band in a wafer after the epitaxy step of the process. (a) $g = (220)$; (b) $g = (1\ -1\ 1)$.

figure 3(a)) than it is 1 cm from it (about 10 nm; figure 3(b)). From these measurements and from the knowledge of the different slip systems in silicon, it is possible to evaluate the number of dislocations that passed through the scanned regions. Of course, this applies only to dislocations with a Burgers vector not parallel to the wafer surface. A 90 nm step corresponds to the glide of about 330 dislocations and a 10 nm step to approximately 40. The density of dislocations along the slip line is then about 3×10^2 per centimetre of slip line. Owing to this low density, these slip lines do not seem to be suitable for TEM study.

2.2.2. Selective etching. As this technique allows a one to one correlation between a mound and a crystal defect, it is possible to have an overview of the defect distribution along a slip band [7]. The samples were etched by Sirtl etch for 10 minutes and then observed by scanning electron microscopy (SEM). The area close to the flat part of the wafer was chosen for those experiments because this region is even more thermally stressed than the rest of the crystal due to laser marks. Some of the long alignments of crystal defects, observed in figure 4(a), are present in the areas where slip lines were spotted before etching. Some of those alignments do not match with visible slip lines. This illustrates the effect of the different slip systems: indeed, four of the 12 slip systems of silicon do not lead to steps on the wafer surface because their Burgers vector is parallel to the (001) plane. Along these alignments, the density of dislocations is heterogeneous. Consider a particular alignment from the border of the wafer towards the centre: there are very few dislocations at the beginning, when we find approximately one dislocation every 30 to 50 nm (figure 4(b)). At the end there are so many mounds that they cannot be distinguished (figure 4(c)). The average defect density evaluated from these observations is around 10^2 per cm of slip line.

In conclusion of this work, it is possible to evaluate the feasibility of a TEM investigation of dislocations in slip bands. Although the average density is too low for TEM study, the etching experiments lead us to expect a sufficient density of dislocations at the end of the slip bands.

Figure 6. Same region as in figure 4, TEM dark field weak beam image (printed in reverse contrast), $g\ -\ g$; $g = (022)$.

2.3. TEM specimen preparation

Plan-view TEM specimens were prepared with the tripod mechanical polishing technique using diamond discs in order to obtain thin bevelled slices of silicon with a thickness of 10 microns on one side and 1 micron on the other. To obtain electron transparency, ion milling was used for approximately 30 minutes. Finally, the TEM observations were made in an electron microscope operated at 200 kV. As the extremity of the slip band is difficult to locate with an optical microscope, many plan-view samples were prepared and observed by TEM until the target was observable in one of them.

3. TEM observations

Figures 5(a) and 5(b) are bright field micrographs of the extremity of an about 10 micron long slip band from the first type of sample, taken from the process lines after the epitaxy step. Slip occurs in different slip planes parallel to each other (see figure 5(b) where the glide planes are edge on). A closer view of the extremity of a slip band can be seen on weak beam dark field micrographs (figure 6); it consists of a pile-up of dislocations parallel to each other. The dislocations at the extremity are quite straight whereas the subsequent dislocations are more and more distorted. The crystallographic characteristics of the slip band and its dislocations were determined by extinction conditions [8]. The slip plane is $(1\ -1\ 1)$; dislocations lie in the $[-1\ 0\ 1]$ direction. At the extremity of the pile-up, perfect dislocations have a $\frac{1}{2}$ [110] Burgers vector. As this Burgers vector lies in the (001) plane, it cannot induce a slip step at the surface of the wafer. Also many cusps can be seen on the dislocations and even dipoles. These dipoles are all along the [011] direction.

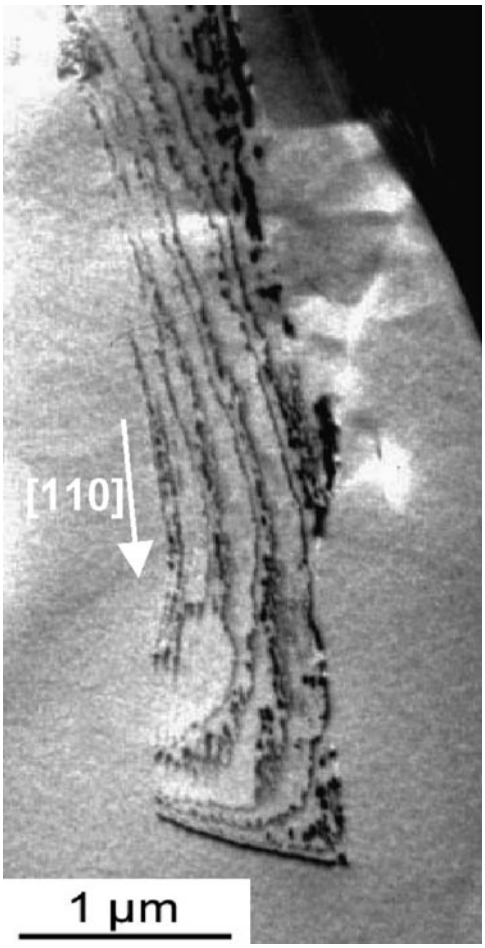

Figure 7. TEM dark field image of a slip band in a wafer that went through the whole process (printed in reverse contrast); $g = (220)$.

The second type of sample has also been studied: dice from wafers that went through the whole process and contained operational devices. These dice were electrically tested and then all layers were chemically or plasma etched to silicon surface. In figure 7, a slip band is observable in a pad region of an electrically good die. Indeed, in this region there are no junctions in the silicon epitaxy layer that can be damaged by the slip band presence. It seems that the dislocations nucleated from the surface of the wafer and then slipped into the crystal. The dislocations are even more distorted than in the previous case and they are also paired. These dislocations are widely dissociated in their $(1\ -1\ 1)$ slip plane according to the reaction $b_1 + b_2 = b_T$ with $b_1 = -1/6\,[121]$, $b_2 = 1/6\,[-2\ -1\ 1]$ and $b_T = -1/2\,[110]$. Again in this case, this Burgers vector parallel to the surface cannot induce a step. Looking closer at the slip band, shearing loops can be seen between the partial dislocations. Inside and outside contrast of these loops were obtained using opposite diffraction conditions, g and $-g$, but keeping the same positive s (deviation from the Bragg reflection position) in figures 8(a) and 8(b). The Burgers vector and line orientation of the loops, as shown schematically in figure 8(c), were determined using the rules listed in [9].

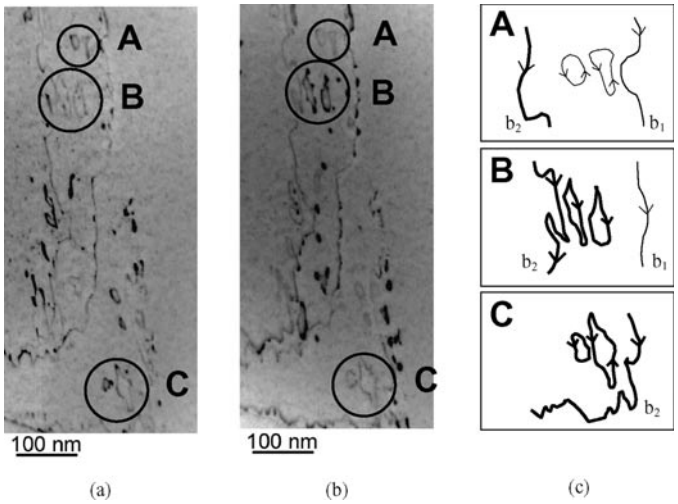

Figure 8. Same region as in figure 6, TEM dark field weak beam image, (a) $g = (220)$, s positive; (b) $g = (-2\ -2\ 0)$, s positive (printed in reverse contrast). (c) Schematic representation of the loops A, B and C; bold line, b_2 dislocations; fine line, b_1 dislocation; line orientation shown by arrows.

4. Discussion

The present results give more information on the structure of the slip bands than the previous work [1–3] as they are concerned with characterization at a microscopic scale. The two configurations observed, weakly dissociated and widely dissociated dislocations, may be related to the different thermo-mechanical treatments of the process.

In both kinds of sample the dislocations are very distorted as cusps, dipoles and shearing loops were observed. It seems that the dislocations encountered obstacles during slip and were pinned up by small defects. These small defects were not yet identified but segregation of dopants or impurities may be suspected. Further investigations are in progress to elucidate this point.

Concerning the nature of the shearing loops, we suggest the following mechanism: a partial dislocation pinned by a small defect leaves behind a shearing loop around the defect. The induced loop must have the same Burgers vector as that of the dislocation that created it and the line orientation of the loop is also related to that of the dislocation. Applying this mechanism to our observations (figures 8(a), 8(b) and 8(c)) it is shown that C loops were left behind by an inward motion of the (b_2) partial. In the same way, the A loops were left by an inward motion of (b_1) dislocations. B loops, which have the same Burgers vector as C loops but an opposite line orientation, are suggested to be left by a backward motion of (b_2) partials during the heat treatments.

References

[1] Hu S M 1977 *J. Vac. Sci. Technol.* **14** 17
[2] Hu S M 1973 *Appl. Phys. Lett.* **22** 261
[3] Hu S M, Klepner S P, Schwenker R O and Seto D K 1976 *J. Appl. Phys.* **47** 4096
[4] Shimizu H, Isomae S, Minowa K, Satoh T and Suzuki T 1998 *J. Electrochem. Soc.* **145** 2523
[5] Bloem J and Goemans A H 1972 *J. Appl. Phys.* **43** 1281

[6] Minowa K and Sumino K 1992 *Phys. Rev. Lett.* **69** 320
[7] Chandler T C 1990 *J. Electrochemical Soc.* **137** 944
[8] Edington J W 1975 *Practical Electron Microscopy in Materials Science* vol 3 (London: Macmillan) p 14
[9] Williams D B and Carter C B 1996 *Transmission Electron Microscopy* vol 3 (New York: Plenum) p 407